Rheol Acta (2010) 49:931–939
DOI 10.1007/s00397-010-0461-x

ORIGINAL CONTRIBUTION

Crystallization of an ethylene-based butene plastomer: the effect of uniaxial extension

Martin Sentmanat · Omar Delgadillo-Velázquez, Savvas G. Hatzikiriakos

Received: 16 December 2009 / Revised: 25 March 2010 / Accepted: 2 May 2010 / Published online: 15 May 2010

Abstract In this paper, the effect of uniaxial extension on the crystallization of an ethylene-based butane plastomer is examined by using rheometry coupled with differential scanning calorimetry (DSC). Uniaxial extension experiments were performed at temperatures below and above the peak melting point of the polyethylene in order to characterize its flow-induced crystallization behavior at extensional rates relevant to processing. The degree of crystallinity of the stretched samples was quantified by DSC, i.e., by analyzing the thermal behavior of samples after stretching. Analysis of the tensile strain-hardening behavior very near the peak melt temperature revealed that crystallization depends on temperature, strain, and strain rate. In addition, it was revealed that a very small window of temperatures spanning just 1–2°C can have a dramatic effect on polymer crystallization. Finally, flow-induced crystallization experiments at temperatures close to the peak melting point have shown the recrystallization of multiple crystalline structures within a polymer matrix, witnessed by double peaks within a narrow window of 89–93°C in the DSC thermographs, with the most demonstrable double peak behavior occurring at a temperature of 91°C, a temperature that is just 1°C cooler than the peak melt temperature of the polymer.

M. Sentmanat
Xpansion Instruments, 1425 Glenoak Dr.,
Tallmadge, OH 44278, USA

O. Delgadillo-Velázquez · S. G. Hatzikiriakos (✉)
Department of Chemical and Biological Engineering,
The University of British Columbia,
Vancouver, Canada
e-mail: hatzikir@interchange.ubc.ca

Keywords Ethylene-based butene plastomer · Flow-induced crystallization · Extensional flow · Double peak in DSC

Introduction

Plastic products are manufactured by deforming the polymer at elevated temperatures into a desired shape. Examples include film blowing, film casting, fiber spinning, and calendaring. Polymers used in these processes include most polyolefins, i.e., linear low-density (LLDPE), low-density (LDPE), and high-density polyethylenes (HDPE). When transitioning from the molten state to the solid state during processing, these polymers undergo crystallization, and as a result, their final mechanical properties heavily depend on the conditions under which crystallization takes place (McHugh 1995; Eder et al. 1990; Kornfield et al. 2002; Janeschitz-Kriegl 2003; Scelsi and Mackley 2008). In fact, the mechanical properties depend heavily on the thermal and deformation histories experienced by the polymer during the crystallization process. For instance, in extruded fibers, the crystals are oriented in the direction of extension, while in films formed by film blowing, the crystals are oriented in the plane of biaxial extension. In both of these applications, the orientation of the crystalline phase enhances the mechanical properties of the final product (Gelfer and Winter 1999). There are examples where formation of crystalline phase might influence negatively the mechanical properties of final products, i.e., crystalline phase skin formation during injection molding.

Polymers such as polyethylene are always semi-crystalline in solid form (Dealy and Wissbrun 1990).

Their crystallization rates at temperatures below the melting point are very high, and it is not possible to cool the polymer rapidly enough to a temperature below the glass transition temperature without substantial crystallization taking place. Under quiescent conditions, the crystallization rate for polyethylenes is usually observed to be zero at the melting temperature and at the glass transition temperature, with a maximum occurring at a temperature in between these two temperatures. However, under flow conditions at temperatures near the melt state, the kinetics of crystallization might significantly change, and it may become a function of deformation history depending on both strain and rate (Kitoko et al. 2003; Hadinata et al. 2006; Dai et al. 2006; Tanner and Qi 2009; Tanner et al. 2009). The type of flow deformation can also play a significant role in affecting crystallization. For example, extensional flow (which is an inherently strong flow) causes molecules to orient and stretch in the direction of extension (as in the case of fiber spinning) facilitating the process of flow-induced crystallization (FIC; Swartjes et al. 2003; Janeschitz-Kriegl 2003; Kornfield et al. 2002; Stadlbauer et al. 2004). Although shear deformations also influence the crystallization behavior of polyethylenes (Monasse 1995; Vleeshouwers and Meijer 1996; Alfonso and Scardigli 1997; Koran and Dealy 1999; Lagasse and Maxwell 1976; Fortenly et al. 1995; Fernandez-Ballester et al. 2009), because these shear flow fields are not typically as strong as extensional flows, very large strains must be generated in order to observe shear flow-induced crystallization.

The main focus of this paper was to study first the rheological behavior of an ethylene-based butane plastomer at temperatures around the point of crystallization/melting and, secondly, the effect of extensional flows on its crystallization. Film blowing and calendaring are two flows that involve significant degrees of extensional flow elements and therefore becomes important to see how extension influences structure formation (crystalline phase formation) in polyethylenes. In addition, the obtained data is very useful to evaluate important flow-induced crystallization models (Doufas et al. 1999, 2000a, b; Tanner et al. 2009; Tanner and Qi 2009).

Experimental

A film-grade ethylene-based butene plastomer Exact™ 3128 from ExxonMobil was studied in this work with a specific interest in its flow-induced crystallization behavior. This polymer has an melt flow index of 1.2, a molecular weight of about 80 kg/mol, and a polydispersity of about 2. Because of the higher degree of crystallization that can be achieved in the solid state, linear polymers are particularly sensitive to extensional flows very near the melt temperature, and for this reason, an ethylene-based butene plastomer resin was selected for this study (Sentmanat and Hatzikiriakos 2004; Sentmanat et al. 2005a).

A Shimadzu DSC-60 calorimeter was used to study the thermal behavior of the plastomer. Measurements were made on samples of about 1–2 mg, sealed in aluminum pans and nitrogen flow. The samples were heated from 30°C to 180°C at a heating rate of 10°C/min in order to determine the melting temperature (T_m) and heat of fusion (ΔH_m). The calorimeter was calibrated periodically for melting temperature and heat flow using indium and zinc as standards.

The linear viscoelastic (LVE) rheological properties of the polymer were characterized in small amplitude oscillatory shear using an Anton Paar rotational rheometer (MCR 501) equipped with circular platens 25 mm in diameter. The polymer was also characterized in simple extension using a model SER2-P SER Universal Testing Platform (Sentmanat 2003, 2004) fixture hosted on the MCR 501. Uniaxial extension experiments were run at various temperatures, strain rates, and strains to examine their effect on the crystallization behavior of the plastomer. In addition, tensile stress relaxation measurements were also performed on the polymer by stopping the uniaxial extension at various levels of strains. As will be discussed later, this type of experiment shows clearly the effect that the extensional strain plays in the crystallization of polymers. Finally, tensile experiments were run at temperatures from ambient up to melting point in order to assess the importance of deformation behavior at temperatures near the peak melting point temperature, T_{m}. As will be further discussed, it is within this range of temperatures near T_{m} that most of the critical crystallization phenomena occur due to the combined effects of molecular mobility and the affinity of the molecule to crystallize. For example, at temperatures well below T_{m}, molecules lose their flexibility or ability to orient and additional crystallization is difficult to achieve, unless significant deformation is imposed.

Melt rheology

Figure 1 contains the rheological master curves for linear viscoelastic shear moduli and the complex viscosity of the plastomer at a reference temperature of 170°C. Small amplitude oscillatory shear experiments were carried out over a wide range of temperatures

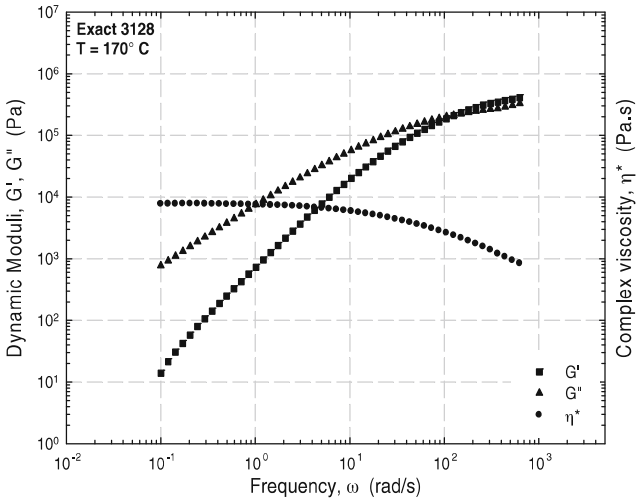

Fig. 1 Linear viscoelastic moduli, G′, G″, and complex viscosity, $|\eta^*(\omega)|$ of the ethylene-based butene plastomer Exact™ 3128 at 170°C

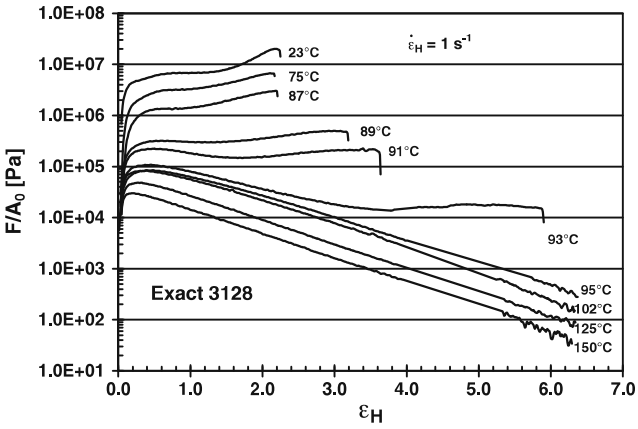

Fig. 3 A series of steady Hencky strain rate uniaxial experiments for the ethylene-based butene plastomer Exact™ 3128 at various temperatures shown in Fig. 2, well below, around, and well above the peak melting point

from 130°C to 230°C at 20°C increments while the time-temperature superposition shift factors were calculated from MATLAB. The superposition of the data was excellent, illustrating the thermorheological simplicity of this plastomer, an observation that is consistent with most linear polymers.

Flow-induced crystallization in uniaxial extension

Figure 2 depicts the melting thermographs of the plastomer obtained from differential scanning calorimetry (DSC) and shows that the onset of melting occurs at about 87°C with the peak melt temperature at 92°C. Figure 3 plots the engineering stress F/A_o (instantaneous tensile force Fdivided by the initial cross-sectional area of the sample) as a function of the Hencky strain ε_H (also known as true strain) for several temperatures shown in Fig. 2 and for a given Hencky strain rate of $\dot{\varepsilon}_H = 1\ s^{-1}$. The top 3 curves from 23°C to 87°C correspond to the solid physical state of the polymer, depicting classic plastic behavior of yielding, necking, and strain hardening to tensile rupture. It should be noted that to control the thermal history of all of the samples at a temperature near the melt state, each test specimen was loaded on the SER fixture and presoaked within the precision Thermo chamber (CTD600) oven of the MCR501 for 5 min at a temperature of 102°C in order to eliminate any residual crystallinity prior to cooling and stretching of the test specimen. Note that a higher presoak temperature was not used in order to avoid excessive melt sagging of the test sample during the presoak period on the SER fixture. Over a range of temperatures from 89°C to 93°C (within the peak melt trough of the DSC thermograph), the material is molten yet experiences a strain-hardening behavior with increasing strain as a result of the onset of FIC. However, at test temperatures beyond the DSC peak melt trough region (95°C and above), there is no evidence of FIC, and as a result, the engineering tensile stress keeps decreasing monotonically with increasing Hencky strain in a manner consistent with classic molten flow behavior of linear polymers. This series of experiments clearly depicts the significant roles that temperature and extensional deformation play in the crystallization of polymers.

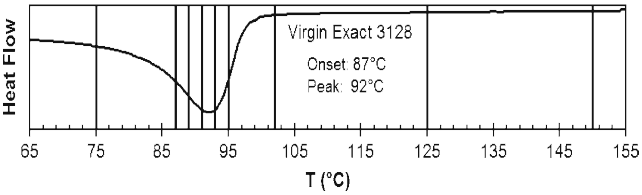

Fig. 2 The thermograph (DSC) of the ethylene-based butene plastomer Exact™ 3128 showing that the onset of melt occurs at 87°C with the melting peak at 92°C

Tensile stress growth coefficient, η_E^+

Figure 4 plots the tensile stress growth coefficient, η_E^+ of the plastomer as a function of the Hencky strain at several Hencky strain rates ranging from 0.01 to 30 s^{-1} and three temperatures, namely, 91°C, 93°C, and 102°C. First, at 102°C, the polymer is in the fully molten state (well above the melting point), and the tensile

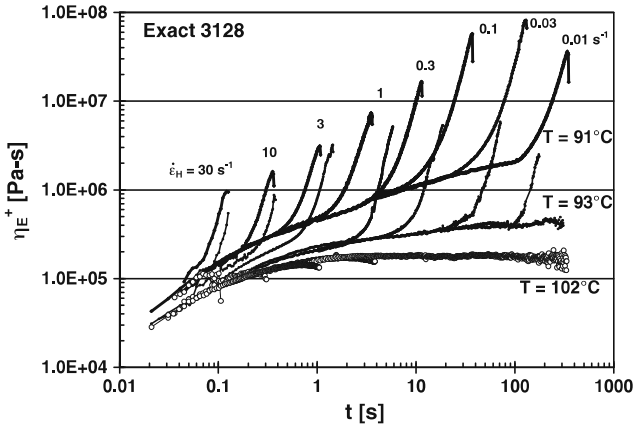

Fig. 4 The tensile stress growth coefficient η_E^+ of the ethylene-based butene plastomer Exact™ 3128 at various temperatures (91°C, 93°C, and 102°C) and Hencky strain rates ranging from 0.01 to 30 s^{-1}

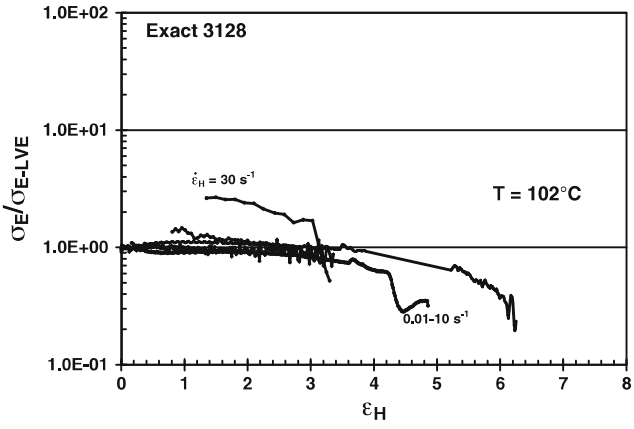

Fig. 5 The tensile stress normalized by the tensile stress from LVE; that is, σ_E/σ_{E-LVE} as a function of the Hencky strain ε_H at 102°C

stress growth coefficient follows the LVE envelope that forms the LVE theory equals three times the linear viscoelastic shear stress growth coefficient, $3\eta^+$, and is typically described by the base curve on which all of the low-strain transient extensional data for all Hencky strain rates tend to collapse. It is noted that there is no sign of strain hardening (defined as a positive stress deviation from the LVE envelope) in a manner consistent with the classic flow behavior of molten linear polymers (Dealy and Wissbrun 1990). At 93°C, although the flow for a given strain rate initially follows along the LVE envelope beyond a critical strain, significant deviations from LVE behavior are observed despite being just 1°C above the peak melt temperature. At all Hencky strain rates (except the smallest of 0.01 s^{-1}), strong strain hardening is observed, which provides clear evidence of FIC. The LVE provides a reasonable indication as to the effect of quiescent crystallization of the bulk polymer, and any strain hardening is due to the FIC. At a temperature of 91°C, just 1°C below the peak melt temperature, the flow for all of the strain rates again exhibits significant deviation from the LVE envelope but at an even earlier onset of critical strain as a result of FIC. Furthermore, the significant shift in the LVE envelope from 93°C to 91°C displays the inherent effect of temperature on the quiescent crystallization state within the bulk polymer that apparently serves to assist or seed the observed FIC behavior. In other words, the underlying crystallinity present in the bulk polymer due to quiescent crystallization prior to sample stretch appears to serve as seed crystallization sites within the polymer matrix brought on by the increased orientation and molecular chain stretch during uniaxial extension, thereby resulting in the observed dramatic flow-induced crystallization behavior. A great similarity is noted between the tensile stress growth coefficient curves plotted in Fig. 4 and the corresponding calculated ones performed by Doufas et al. (1999); therefore, such sets of data can be used to fit parameters of such FIC models.

These strain-hardening effects can be seen more clearly if one plots the data of Fig. 4 in terms of a relative deviation from LVE behavior as the ratio of the instantaneous tensile stress to the tensile stress from the LVE envelope; in other words, σ_E/σ_{E-LVE}. The data of Fig. 4 for all three temperatures of 102°C, 93°C, and 91°C are plotted in Figs. 5, 6, and 7, respectively, in terms of relative strain hardening ratio as σ_E/σ_{E-LVE} vs. the Hencky strain, ε_H. Figure 5 shows the data at 102°C where the polymer is 10°C above its peak melt

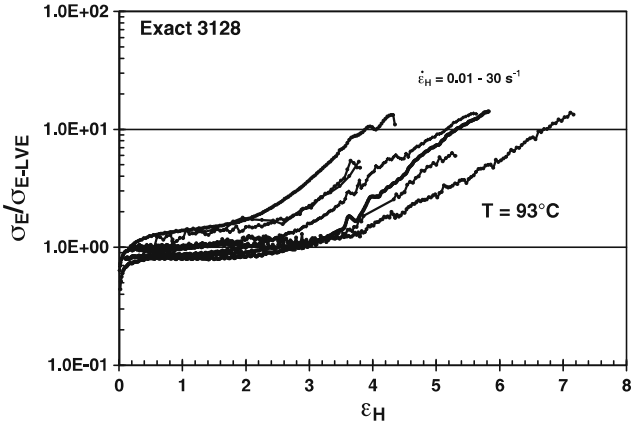

Fig. 6 The tensile stress normalized by the tensile stress from LVE, that is, σ_E/σ_{E-LVE} as a function of the Hencky strain ε_H at 93°C

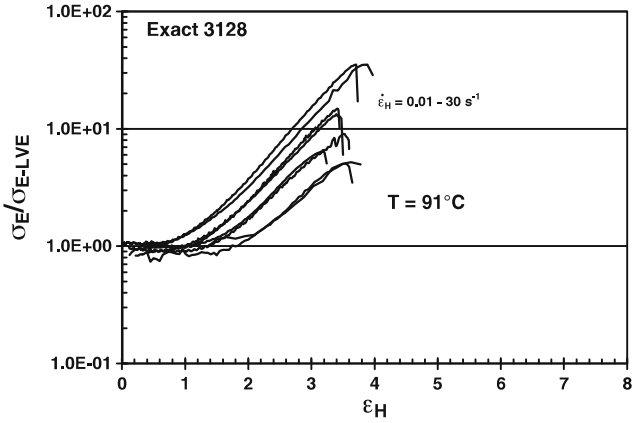

Fig. 7 The tensile stress normalized by the tensile stress from LVE, that is, σ_E/σ_{E-LVE} as a function of the Hencky strain ε_H at 91°C

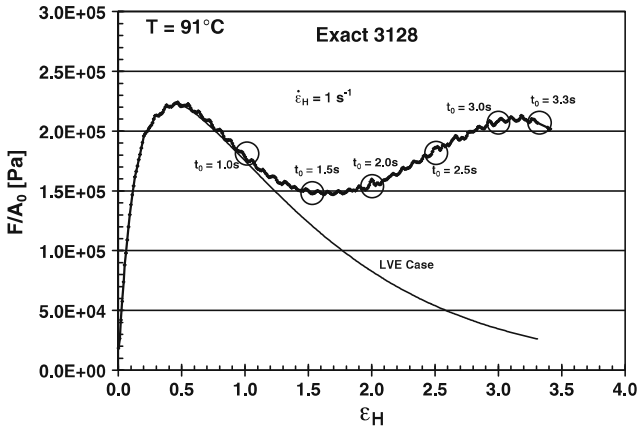

Fig. 8 A constant Hencky strain rate ($\dot{\varepsilon}_H = 1\ s^{-1}$) uniaxial experiment for the ethylene-based butene plastomer Exact™ 3128 at 91°C

temperature. The ratio σ_E/σ_{E-LVE} remains around a value of 1 at all Hencky strain rates prior to sample failure in a manner consistent with the classic behavior of a linear polymer melt, indicating that FIC is absent. As shown in Fig. 6, at 93°C (that is 1°C above the peak melting point), the effect of FIC is significant. The ratio σ_E/σ_{E-LVE} increases well above a value of 1 (the definition of strain hardening) for all Hencky strain rates beyond a critical Hencky strain of about 2. As depicted in Fig. 7, at 91°C (only 1°C below the peak melting point), the effect of FIC is even more pronounced. The ratio σ_E/σ_{E-LVE} increases sharply beyond a critical Hencky strain just above 1. In general, the critical Hencky strain at the onset of strain-hardening behavior appears to somewhat decrease with increasing Hencky strain rate. Furthermore, the discernable trends in the data from Figs. 4, 6, and 7 appear to suggest that the effects of quiescent crystallization and FIC on the bulk polymer rheology are somewhat separable, which implies that for a given temperature condition from a potential constitutive modeling perspective, the effects of quiescent crystallization can be modeled primarily as a function of time affecting the linear viscoelastic bulk rheological properties, while the effects of FIC can be modeled primarily as a function of strain and rate, thereby affecting the non-linear viscoelastic bulk rheological properties of a given polymer system.

Tensile stress relaxation after imposition of steady uniaxial extension

Figure 8 contains a plot of the engineering stress F/A_o (instantaneous tensile force Fdivided by the initial cross-sectional area of the sample) as a function of the Hencky strain ε_H at a temperature of 91°C and a Hencky strain rate of $\dot{\varepsilon}_H = 1\ s^{-1}$. As discussed before and witnessed by the data in Fig. 8, at the early stages of stretching, the polymer appears to remain in a molten state, displaying little deviation from the LVE envelope; however, at strains greater than 1, FIC crystallization appears evident from the inflection and sudden increase of the engineering tensile stress curve. In order to characterize the stress relaxation behavior of the polymer after the onset of FIC, cessation of extension experiments (in which the stretching deformation is suddenly stopped at a predetermined strain) were performed on samples after a predetermined strain imposition corresponding to various points along the curve in Fig. 8, i.e., after 1 s when the polymer exhibits near-LVE behavior; after 1.5, 2, 2.5, and 3 s during the FIC process; and finally, at a time 3.3 s immediately prior to the onset of sample rupture.

The results for these relaxation experiments are plotted in Fig. 9, which depicts the instantaneous stress as a function of time. As described earlier, each test specimen was loaded on the SER fixture and presoaked within the CTD oven of the MCR501 for a period of 5 min at a temperature of 102°C in order to eliminate any residual crystallinity prior to cooling and stretching of the test specimen at the test temperature of 91°C. When the stretching is stopped at the early stages of the experiment (after 1 s) the polymer is still in a molten state and stress relaxation occurs normally as shown by exponential decay in the tensile stress. However, this is not the case upon the onset of FIC at cessation times greater than 1 s. As seen from Fig. 9, the tensile stress shows no such exponential decay but rather tends to approach an equilibrium stress as in the case of a rubber-like material. At higher cessation strains corresponding

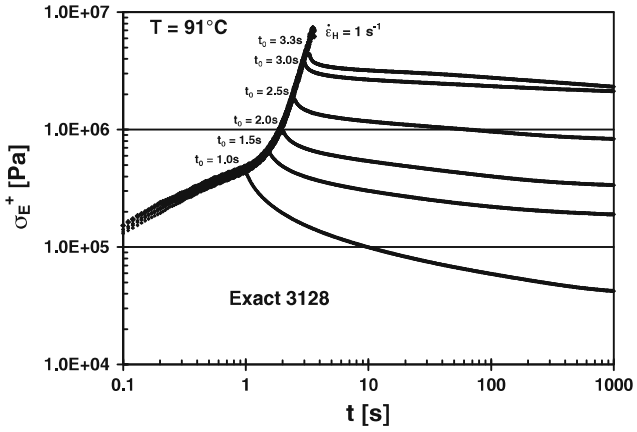

Fig. 9 A series of tensile stress relaxation after imposition of a constant Hencky strain rate ($\dot{\varepsilon}_H = 1\ s^{-1}$) uniaxial experiments for the ethylene-based butene plastomer Exact™ 3128 at 91°C. Note that the tensile stress growth experiment was stopped at various times ranging from 1 to 3.5 s as indicated also in Fig. 8

to the second characteristic peak in Fig. 8, the sample appears to approach a limiting elastic behavior prior to the onset of a sample rupture. Finally, at times beyond the second maximum (roughly for times greater than 3 s), the relaxation becomes abnormal due to the onset of an extensional instability or necking failure that has been previously described in the literature with respect to a Considère criterion (McKinley and Hassager 1999; Sentmanat et al. 2005b).

Thermal (DSC) analysis of stretched samples

In order to assess the degree of crystallinity of the samples undergoing FIC during uniaxial extension experiments with the SER, test specimens were prepared by quickly opening the oven chamber upon completion of an extension experiment and by rapidly quenching the free surfaces of the stretched sample with a water spray. Once the samples had solidified, they were removed from the SER and then prepared for DSC characterization as previously described. Using DSC analysis to determine the heat of melting values, the percent of crystallinity, X, for each sample was calculated using the following expression: $X\,(\%) = \Delta H_m / \Delta H_{m(100\%\text{cryst.PE})}$, where ΔH_m is the heat of the melting value of the sample analyzed with DSC, and $\Delta H_{m(100\%\text{cryst.PE})} = 279 J/g$ is the heat of melting value for 100% purely crystalline polyethylene reported in the literature (Alamo et al. 1997). It should be noted that each SER sample prepared for DSC characterization was stretched to a point immediately prior to sample rupture to a maximum Hencky strain of just above 3 in order to prevent the sample from recoiling and recovering from the imposed uniaxial extension deformation, thereby "locking in" the molecular orientation and state of FIC within the bulk polymer. Again, in order to control the thermal history of all the stretched samples, each test specimen was loaded on the SER fixture and pre-soaked within the CTD oven of the MCR501 for a period of 5 min at a temperature of 102°C in order to eliminate any residual crystallinity prior to cooling and stretching of the test specimen at a test temperature near the melt state.

Figure 10 shows a series of DSC thermographs for the m-LLDPE samples stretched at 93°C at Hencky strain rates up to 3 s^{-1}. From the analysis of the DSC thermographs, it can be concluded that polymer crystallinity increases from 20.8% for an unstretched sample to about 25.2% for samples stretched at high Hencky strain rates. As depicted in the DSC thermographs in Fig. 11, at 91°C, the crystallinity values obtained were even higher and values up to 29% were observed. With respect to Fig. 11, it is worth noting that in addition to the typical single-peak DSC thermograph melting troughs similarly observed at the higher temperature, double peaks are clearly evident in the thermograph melting troughs for SER samples that were stretched at higher Hencky strain rates (>0.3 s^{-1}) at 91°C. Such double peaks have also been observed in the past for the flow-induced crystallization studies of a high-density polyethylene (Fortenly et al. 1995) as well as for crystallization behaviour of a polyaryl ether ketone; (Konnecke 1992). In general, a double peak in a DSC curve is typically attributed to recrystallization of multiple crystalline structures within a polymer

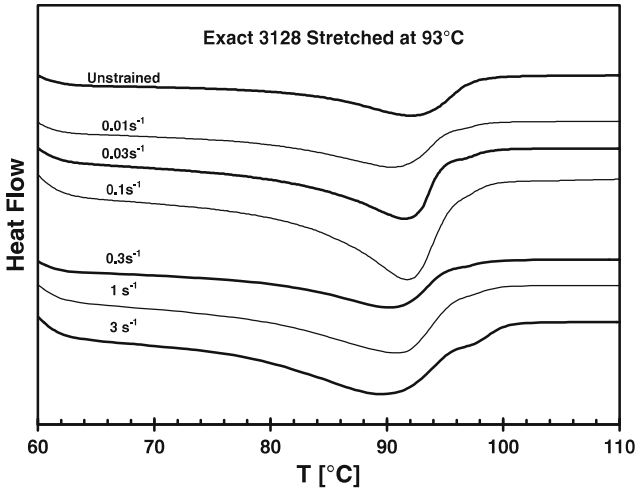

Fig. 10 DSC thermographs for samples first soaked at 102°C and subsequently stretched at various Hencky strain rates at 93°C before being quenched

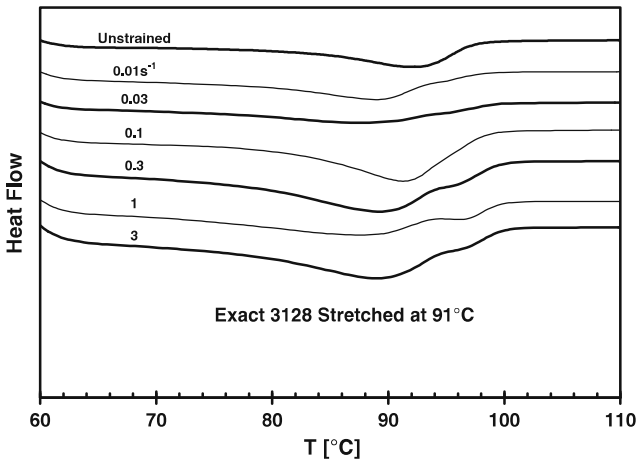

Fig. 11 DSC thermographs for samples first soaked at 102°C and subsequently stretched at various Hencky strain rates at 91°C before being quenched

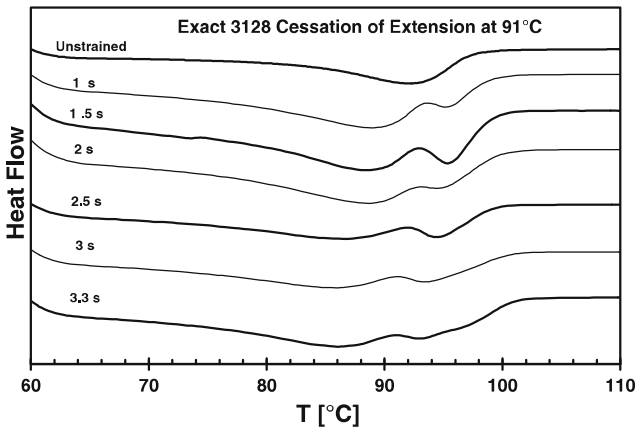

Fig. 12 DSC thermographs for samples first soaked at 102°C and subsequently stretched at the Hencky strain rate of 1 s^{-1} for a specified time (indicated on the curves from 1 to 3.3 s) at 91°C before being quenched

matrix during the temperature ramp sequence or as a result of improper packing (typically an issue with fiber samples) during DSC sample preparation. The fact that the SER samples were not of an acute or fiber-like aspect ratio and that the double peaks appear only for samples stretched and crystallized at a temperature around 91°C, improper DSC sample preparation can thereby be eliminated as a cause for such experimental observations; in other words, these double peaks do not appear to be experimental artifacts. Hence, these data appear to indicate that the stretching of the Exact™ 3128 polymer sample near its peak melt temperature may have produced a different type of crystalline structure within the polymer matrix formed as a result of flow-induced crystallization, in addition to the normal crystalline structure typically produced as a result of quiescent crystallization.

These double peaks are further witnessed in the DSC analysis of the samples collected from the tensile stress relaxation experiments used to generate the stress relaxation curves in Fig. 9 (Fig. 12). Upon completion of each tensile relaxation experiment in Fig. 9, each sample was rapidly quenched and prepared for DSC characterization as previously described. Similar to the double peaks observed at the higher rates in Fig. 11, double peaks in the thermograph melt troughs are clearly evident for all of the samples having undergone stretch and relaxation after an imposed Hencky strain rate of 1 s^{-1}. Furthermore, samples analyzed with DSC after extensional experiments at other temperatures have shown that these double peaks in the thermograph melt trough appear only at temperatures very near the peak melting point of the polymer. This is evidenced by the results depicted in Fig. 13 that present DSC thermographs for rapidly quenched test samples having undergone uniaxial extension deformation at a Hencky strain rate of 1 s^{-1}, spanning a temperature range from 25°C to 150°C. Double peaks in the thermograph melt trough appear only for those samples stretched at temperatures from 89°C to 93°C with this phenomenon being most demonstrable at a stretching temperature of 91°C as clearly illustrated by the data in Figs. 11 and 12. Hence, these DSC results together with the extensional data from Figs. 4, 6, and 7 appear to indicate that the effects of quiescent crystallization and FIC are separable from a mechanistic as well as a molecular structural standpoint.

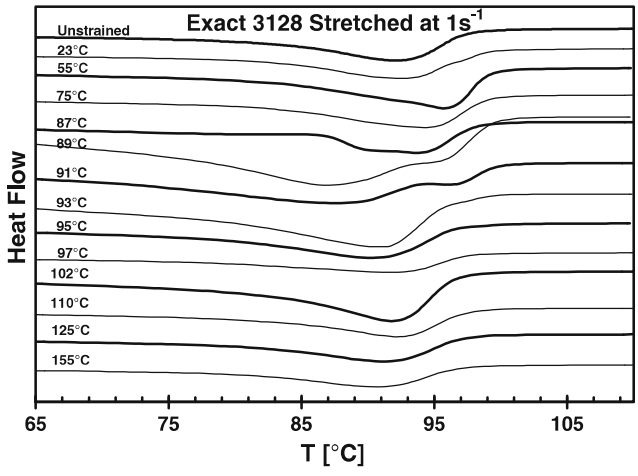

Fig. 13 DSC thermographs for samples first soaked at 102°C and subsequently stretched at the Hencky strain rate of 1 s^{-1} and various temperatures from 23°C to 150°C before being quenched

Conclusions

The extensional behavior of an ethylene-based butane plastomer was characterized over a broad range of temperatures (well above, well below, and around its peak melt temperature) and Hencky strain rates. It was shown that FIC occurs over a range of temperatures near the DSC peak melt temperature. Analysis of the tensile strain-hardening behavior very near the peak melt temperature revealed a temperature and strain dependence on the FIC behavior. The tensile stress growth coefficient revealed that the critical FIC behavior of the plastomer occurs in a significant way over a span of just 1°C above and below the peak melt temperature. Cessation of extension experiments very near the peak melt temperature revealed the retardation effect that FIC has on the stress relaxation behavior of the crystallizing melt. These results demonstrate the significant role that extensional deformation plays in the occurrence and degree of crystallization of polymer melts relevant to the polymer processing industry. Finally, flow-induced crystallization experiments at temperatures close to the peak melting point have shown the recrystallization of multiple crystalline structures within a polymer matrix as witnessed by double peaks in DSC thermograph melt troughs over a very narrow window of temperatures from 89°C to 93°C with this observed phenomenon being most demonstrable at 91°C, a temperature that is just 1°C cooler than the peak melt temperature of the polymer. The experimental results presented here have shown that crystallization is a complex process that heavily depends on time, temperature, strain, and rate and certainly on the type of polymer undergoing stretch.

Acknowledgements Financial assistance from the Natural Sciences and Engineering Research Council (NSERC) of Canada is gratefully acknowledged.

References

Alamo RG, Graessley WW, Krishnamoorti Lohse DJ, Londono JD, Mandelkern L, Stehling FC, Wignall GD (1997) Small angle neutron scattering investigations of melt miscibility and phase segregation in blends of linear and branched polyethylenes as a function of the branch content. Macromolecules 30:561–572

Alfonso GC, Scardigli P (1997) Melt memory effects in polymer crystallization. Macromol Symp 118:323–328

Dai S-C, Qi F, Tanner RI (2006) Strain and strain-rate formulation for flow-induced crystallization. Polym Eng Sci 46:659–669

Dealy JM, Wissbrun KF (1990) Melt rheology and its role in plastics processing—theory and applications. Van Nostrand Reinhold, New York

Doufas AK, Dairanieh IS, McHugh AJ (1999) A continuum model for flow-induced crystallization of polymer melts. J Rheol 43:85–109

Doufas AK, McHugh AJ, Miller C (2000a) Simulation of melt spinning including flow-induced crystallization. Part I. Model development and predictions. J Non-Newton Fluid Mech 92:27–66

Doufas AK, McHugh AJ, Miller C, Immaneni A (2000b) Simulation of melt spinning including flow-induced crystallization. Part II. Quantitative comparisons with industrial spinline data. J Non-Newton Fluid Mech 92:81–103

Eder G, Janeschitz-Kriegl H, Liedauer S (1990) Crystallization processes in quiescent and moving polymer melts under heat transfer conditions. Prog Polym Sci 15:629–714

Fernandez-Ballester L, Thurman DW, Kornfield JA (2009) Real-time depth sectioning: isolating the effect of stress on structure development in pressure-driven flow. J Rheol 53: 1229–1254

Fortenly I, Kovarova J, Kovar J (1995) Flow-induced crystallization of high-density polyethylene. Collect Czechoslov Chem Commun 60:1733–1740

Gelfer MY, Winter HH (1999) Effect of branch distribution on rheology of LLDPE during early stages of crystallizattion. Macromolecules 32:8974–8981

Hadinata C, Gabriel C, Ruellmann M, Kao N, Laun HM (2006) Shear-induced crystallization of PB-1 up to processing-releant shear rates. Rheol Acta 45:539–546

Janeschitz-Kriegl H (2003) How to understand nucleation in crystallizing polymer melts under real processing conditions. Colloid Polym Sci 281:1157–1171

Kitoko V, Keentok M, Tanner RI (2003) Study of shear and elongational flow of solidifying polypropylene melt for low flow deformation rates. Korea–Australia Rheol J 15: 63–73

Konnecke K (1992) Crystallization of poly(aryl ether ketones). Die Angewandte Makromolekulare Chemie 198:15–29

Koran F, Dealy JM (1999) A high pressure sliding plate rheometer for polymer melts. J Rheol 43:1279–1290

Kornfield JA, Kumaraswamy G, Issaian AM (2002) Recent advances in understanding flow effects on polymer crystallization. Ind Eng Chem Res 41:6383–6392

Lagasse RR, Maxwell B (1976) An experimental study of the kinetics of polymer crystallization during Shear flow. Polym Eng Sci 16:189–199

McHugh AJ (1995) Flow induced crystallization in polymers. In: Lyngaae-Jorgenson J, Sandergaard K (eds) Rheo-physics of multiphase polymeric systems. Technomic Publishing Co., Lancaster, pp 227–267

McKinley GH, Hassager O (1999) The considère condition and rapid stretching of linear and branched polymer melts. J Rheol 43:1195–1212

Monasse B (1995) Nucleation and anisotropic crystalline growth of polyethylene under shear. J Mater Sci 30:5002–5012

Sentmanat ML (2003) Dual windup extensional rheometer. US Patent 6,578,413

Sentmanat ML (2004) Miniature universal testing platform: from extensional melt rheology to solid-state deformation behavior. Rheol Acta 43:657–669

Sentmanat ML, Hatzikiriakos SG (2004) Mechanism of gross melt fracture elimination in the extrusion of polyethylenes in the presence of boron nitride. Rheol Acta 43:624–633

Sentmanat M, Muliawan EB, Hatzikiriakos SG (2005a) Fingerprinting the processing behavior of polyethylenes from transient extensional flow and peel experiments in the melt state. Rheol Acta 44:1–15

Sentmanat M, Wang BN, McKinley GH (2005b) Measuring the transient extensional rheology of polyethylene melts using the SER universal testing platform. J Rheol 49:585–606

Scelsi L, Mackley MR (2008) Rheo-optic flow-induced crystallization of polypropylene and polyethylene within confined entry–exit flow geometries. Rheol Acta 47:895–908

Stadlbauer M, Janeschitz-Kriegl H, Eder G, Ratajski E (2004) New extensional rheometer for creep flow at high tensile stress. Part II. Flow induced nucleation for the crystallization of iPP. J Rheol 48:631–639

Swartjes FHM, Pters GWM, Rastogi S, Mejer HEH (2003) Stress induced crystallization in elongational flow. Intern Polym Proc 18:53–66

Tanner RI, Qi F (2009) Stretching, shearing and solidification. Chem Eng Sci 64:4576–4579

Tanner RI, Hadimata C, LeeWo D (2009) Behaviour of a simple crystallization model in tube and channel flow. Rheol Acta 48:499–507

Vleeshouwers S, Meijer HEH (1996) A rheological study of stress induced crystallization. Rheol Acta 35:391–399